JLAB-THY-10-1165

Hypernuclei in the quark-meson coupling model

K. Tsushima* and P. A. M. Guichon†

*Thomas Jefferson Lab., 12000 Jefferson Ave., Newport News, VA 2 3606, USA
†SPhN-DAPNIA, CEA Saclay, F91191 Gif sur Yvette, France

Abstract. We present results of hypernuclei calculated in the latest quark-meson coupling (QMC) model, where the effect of the mean scalar field in-medium on the one-gluon exchange hyperfine interaction, is also included self-consistently. The extra repulsion associated with this increased hyperfine interaction in-medium completely changes the predictions for Σ hypernuclei. Whereas in the earlier version of QMC they were bound by an amount similar to Λ hypernuclei, they are unbound in the latest version of QMC, in qualitative agreement with the experimental absence of such states.

Keywords: Quark-meson coupling model, Hypernuclei, color magnetic hyperfine interaction
PACS: 12.39.-x, 24.85.+p, 21.80.+a, 21.65.Qr

INTRODUCTION

The study of Λ hypernuclei has provided us with important information on the properties of Λ in a nuclear medium and the effective Λ-N interaction [1]. However, the situation for Σ and Ξ hypernuclei is quite different. The special case of ${}^{4}_{\Sigma}$He aside, there is no experimental evidence for any Σ hypernuclei [2], despite extensive searches. It seems likely that the Σ-nucleus interaction is somewhat repulsive and that there are no bound Σ hypernuclei beyond A=4. In the case of the Ξ, the experimental situation is very challenging, but we eagerly await studies of Ξ hypernuclei with new facilities at J-PARC and GSI-FAIR.

To understand further the properties of hypernuclei, we have used the latest version of the quark-meson coupling (QMC) model [3], which will be referred to as QMC-III, and computed the single-particle energies [4]. (The earliest version of QMC will be referred to as QMC-I, where QMC-II [5] also exists.) The major improvement in the QMC-III model is the inclusion of the effect of the medium on the color-hyperfine interaction. This has the effect of increasing the splitting between the Λ and Σ masses as the density rises. This is the prime reason why our results yield no middle and heavy mass Σ hypernuclei [4].

The QMC model was created to provide insight into the structure of nuclear matter, starting at the quark level [6, 7]. Nucleon internal structure was modeled by the MIT bag, while the binding was described by the self-consistent couplings of the confined light quarks (u, d) (not s nor heavier quarks!) to the scalar-σ and vector-ω meson fields generated by the confined light quarks in the other "nucleons". The self-consistent response of the bound light quarks to the mean σ field leads to a novel saturation mechanism for nuclear matter, with the enhancement of the lower components of the valence Dirac quark wave functions. The direct interaction between the light quarks and the scalar σ field is the key of the model, which induces the *scalar polarizability* at the

nucleon level, and generates the nonlinear scalar potential (effective nucleon mass), or the density (σ-field) dependent σ-nucleon coupling. The model has opened tremendous opportunities for the studies of finite nuclei and hadron properties in a nuclear medium (in nuclei), based on the quark degrees of freedom [7].

HYPERONS IN NUCLEAR MATTER

Since the coupling constants of the light quarks (u,d) and σ, ω, and ρ fields are the same for all the light quarks in any hadrons in QMC, the model can treat the interactions in a systematic, unified manner. In particular, the scalar potentials (in-medium mass minus free mass) for hadrons in QMC-I have turned out to be proportional to the light quark number in a hadron — the light quark number counting rule [8]. This is shown in the left panel in Fig. 1.

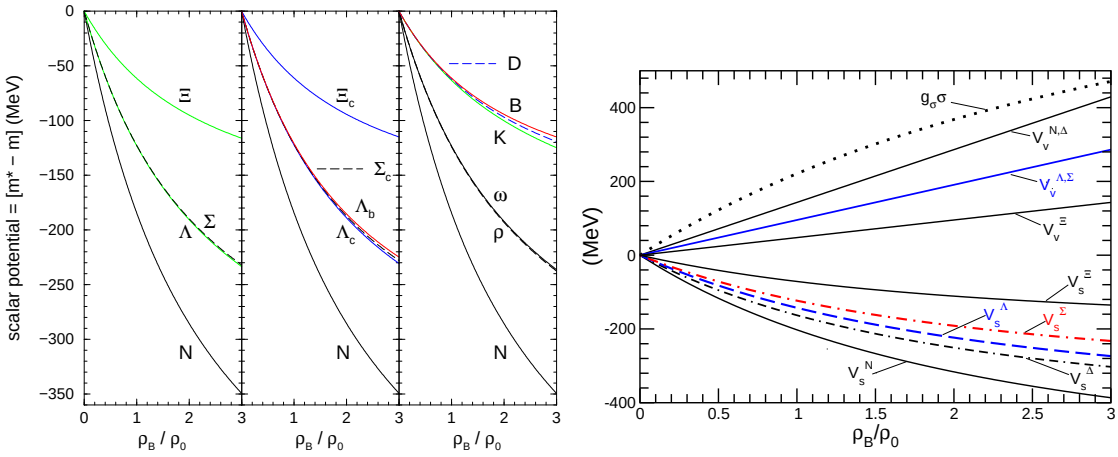

FIGURE 1. Scalar potentials in QMC-I (left panel) [8], and scalar (V_S) and vector (V_V) potentials in QMC-III (right panel) [4], in symmetric nuclear matter. The vector potentials are the same for both QMC-I and QMC-III, proportional to the light quark number in a hadron, and liner as a function of baryon density.

As one can see from the left panel in Fig. 1, the attractive scalar potentials felt by the Λ and Σ are nearly the same. Since the repulsive vector potential is proportional exactly to the light quark number in QMC, the total, nonrelativistic potentials felt by the Λ and Σ are very similar. Thus, as in usual SU(3)-based relativistic mean field models, this naturally led to predict the existence of bound Σ hypernuclei in QMC-I [9], with the similar amount with that of the Λ, despite of some deviations due to the $\Lambda-\Sigma$ channel coupling and phenomenologically introduced Pauli blocking effect at the quark level [9].

However, this difficulty, which contradicts to the experimental observations, is resolved in QMC-III [4]. It is the self-consistent inclusion of the color-hyperfine interaction in a nuclear medium that resolves this difficulty. (Based on the quark and gluon dynamics!) By this color-hyperfine interaction in the nuclear medium, the scalar potential for the Λ gets more attraction, while that for the Σ gets less attraction. (Similarly,the scalar potential for the Δ becomes less attractive than that for the nucleon.) The scalar

(V_S) and vector (V_V) potentials calculated in QMC-III in symmetric nuclear matter are shown in the right panel in Fig. 1.

Explicit expressions for the effective masses (in-medium masses) in QMC-III are,

$$\begin{aligned}
M_N(\sigma) &= M_N - g_\sigma\sigma \\
&\quad + \left[0.002143 + 0.10562R_N^{free} - 0.01791\left(R_N^{free}\right)^2\right](g_\sigma\sigma)^2, \qquad (1)\\
M_\Delta(\sigma) &= M_\Delta - \left[0.9957 - 0.22737R_N^{free} + 0.01\left(R_N^{free}\right)^2\right] g_\sigma\sigma \\
&\quad + \left[0.0022 + 0.1235R_N^{free} - 0.0415\left(R_N^{free}\right)^2\right](g_\sigma\sigma)^2, \qquad (2)\\
M_\Lambda(\sigma) &= M_\Lambda - \left[0.6672 + 0.04638R_N^{free} - 0.0022\left(R_N^{free}\right)^2\right] g_\sigma\sigma \\
&\quad + \left[0.00146 + 0.0691R_N^{free} - 0.00862\left(R_N^{free}\right)^2\right](g_\sigma\sigma)^2, \qquad (3)\\
M_\Sigma(\sigma) &= M_\Sigma - \left[0.6653 - 0.08244R_N^{free} + 0.00193\left(R_N^{free}\right)^2\right] g_\sigma\sigma \\
&\quad + \left[0.00064 + 0.07869R_N^{free} - 0.0179\left(R_N^{free}\right)^2\right](g_\sigma\sigma)^2, \qquad (4)\\
M_\Xi(\sigma) &= M_\Xi - \left[0.3331 + 0.00985R_N^{free} - 0.00287\left(R_N^{free}\right)^2\right] g_\sigma\sigma \\
&\quad + \left[-0.00032 + 0.0388R_N^{free} - 0.0054\left(R_N^{free}\right)^2\right](g_\sigma\sigma)^2, \qquad (5)
\end{aligned}$$

where, the bag radius in free sapce, R_N^{free}, has been taken 0.8 fm for numerical calculations, but the results are quite insensitive (c.f. Fig. 1 of Ref. [3]) to this parameter.

HYPERNUCLEI

In this section we present the results for hypernuclei calculated in QMC-III. Details are given in Ref. [4]. To calculate the hyperon levels, we use a relativistic shell model, and generate the shell model core using the Hartree approximation. The free space meson nucleon coupling constants are, $g_\sigma^2 = 8.79m_\sigma^2$, $g_\omega^2 = 4.49m_\omega^2$ and $g_\rho^2 = 3.86m_\rho^2$, with m_σ = 700 MeV, m_ω = 770 MeV and m_ρ = 780 MeV [3]. Once we have the shell model core wave functions, we use the more sophisticated Hartree-Fock couplings for the hyperon. In a previous study of high central density neutron stars [3], where the hyperon population is large enough that their exchange terms matter, we found that the Hartree-Fock couplings, $g_\sigma^2 = 11.33m_\sigma^2$, $g_\omega^2 = 7.27m_\omega^2$ and $g_\rho^2 = 4.56m_\rho^2$, gave a satisfactory phenomenology. So, for the hyperons we use these couplings. (See also Eqs. (3) - (5)).

Before discussing the results in detail, we first note the remarkable agreement between the calculated (-26.9 MeV in $^{209}_{\Lambda}$Pb) and the experimental (-26.3 ± 0.8 MeV in $^{208}_{\Lambda}$Pb) binding energy of the Λ in the $1s_{1/2}$ level. In our earlier work the Λ was overbound by

12 MeV and we needed to add a phenomenological correction which we attributed to the Pauli effect at the quark level. This correction is not needed when we use Hartree-Fock, rather than Hartree, coupling constants.

Already at this stage the binding of the Σ^0 in the $1s_{1/2}$ level of ${}^{209}_{\Sigma^0}$Pb is just a few MeV – a major improvement over the earlier QMC-I results. However, there is an additional piece of physics which really should be included and which goes beyond the naive description of the intermediate range attraction in terms of σ exchange. In particular, the energy released in the two-pion exchange process, N $\Sigma \rightarrow$ N $\Lambda \rightarrow$ N Σ, because of the Σ–Λ mass difference, reduces the intermediate range attraction felt by the Σ hyperon. In Ref. [9] this was modeled by introducing an additional vector repulsion for a Σ hyperon. Following the same procedure, we replace $g^{\Sigma}_{\omega}\omega(r)$ by $g^{\Sigma}_{\omega}\omega(r)+\lambda_{\Sigma}\rho_B(r)$, with $\lambda_{\Sigma}=50.3$ MeV-fm^3, as determined in Ref. [9] by the comparison with the more microscopic model of the Jülich group [10].

Our results are presented in Tables 1 and 2. The overall agreement with the experimental energy levels of Λ hypernuclei across the periodic table is quite good. The discrepancies which remain may well be resolved by small effective hyperon-nucleon interactions which go beyond the simple, single-particle shell model. Once again, we stress the very small spin-orbit force experienced by the Λ, which is a natural property of the QMC model [9].

TABLE 1. Single-particle energies (in MeV) for ${}^{17}_{Y}$O, ${}^{41}_{Y}$Ca and ${}^{49}_{Y}$Ca hypernuclei ($Y=\Lambda,\Xi^0$). Neither the Σ^0 nor the Σ^+ is bound in strong interaction. The experimental data are taken from Ref. [1] (Table 11) for ${}^{16}_{\Lambda}$O and from Ref. [11] for ^{40}Ca.

	${}^{16}_{\Lambda}$O(Exp.)	${}^{17}_{\Lambda}$O	${}^{17}_{\Xi^0}$O	${}^{40}_{\Lambda}$Ca(Exp.)	${}^{41}_{\Lambda}$Ca	${}^{41}_{\Xi^0}$Ca	${}^{49}_{\Lambda}$Ca	${}^{49}_{\Xi^0}$Ca
$1s_{1/2}$	-12.42 $\pm$0.05 $\pm$0.36	-16.2	-5.3	-18.7 $\pm$1.1	-20 .6	-5.5	-21.9	-9.4
$1p_{3/2}$		-6.4	—		-13.9	-1.6	-15.4	-5.3
$1p_{1/2}$	-1.85 $\pm$0.06 $\pm$0.36	-6.4	—		-13.9	-1.9	-15.4	-5.6

TABLE 2. Same as table 1 but for ${}^{91}_{Y}$Zr and ${}^{209}_{Y}$Pb hypernuclei. The experimental data are taken from Ref. [1] (Table 13).

	${}^{89}_{\Lambda}$Yb(Exp.)	${}^{91}_{\Lambda}$Zr	${}^{91}_{\Xi^0}$Zr	${}^{208}_{\Lambda}$Pb(Exp.)	${}^{209}_{\Lambda}$Pb	${}^{209}_{\Xi^0}$Pb
$1s_{1/2}$	-23.1 $\pm$0.5	-24.0	-9.9	-26.3 $\pm$0.8	-26.9	-15.0
$1p_{3/2}$		-19.4	-7.0		-24.0	-12.6
$1p_{1/2}$	-16.5 $\pm$4.1 ($1p$)	-19.4	-7.2	-21.9 $\pm$0.6 ($1p$)	-24.0	-12.7
$1d_{5/2}$		-13.4	-3.1	—	-20.1	-9.6
$2s_{1/2}$		-9.1	—	—	-17.1	-8.2
$1d_{3/2}$	-9.1 $\pm$1.3 ($1d$)	-13.4	-3.4	-16.8 $\pm$0.7 ($1d$)	-20.1	-9.8
$1f_{7/2}$		-6.5	—	—	-15.4	-6.2
$2p_{3/2}$		-1.7	—	—	-11.4	-4.2
$1f_{5/2}$	-2.3 $\pm$1.2 ($1f$)	-6.4	—	-11.7 $\pm$0.6 ($1f$)	-15.4	-6.5
$2p_{1/2}$		-1.6	—	—	-11.4	-4.3
$1g_{9/2}$		—	—	—	-10.1	-2.3
$1g_{7/2}$		—	—	-6.6 $\pm$0.6 ($1g$)	-10.1	-2.7

There are no entries for the Σ-hyperon because neither the Σ^+ nor the Σ^0 is bound to a finite nucleus in strong interaction. This absence of bound Σ hypernuclei constitutes a major advance over QMC-I. We stress that this is a direct consequence of the enhancement of the hyperfine interaction (that splits the masses of the Σ and Λ hyperons) by the mean scalar field in-medium. It is especially interesting to examine the effective non-relativistic potential felt by the Σ^0 in a finite nucleus. For example, we show in Fig. 2 the Σ^0 potentials in ${}^{41}_{\Sigma^0}$Ca and ${}^{209}_{\Sigma^0}$Pb. In ${}^{41}_{\Sigma^0}$Ca, the vector repulsion from the ω wins in the center, with the potential being as large as $+20$ to $+30$ MeV there, while the scalar attraction wins in the surface with the potential reaching approximately -10 MeV around 4fm. For ${}^{209}_{\Sigma^0}$Pb, the trend is similar.

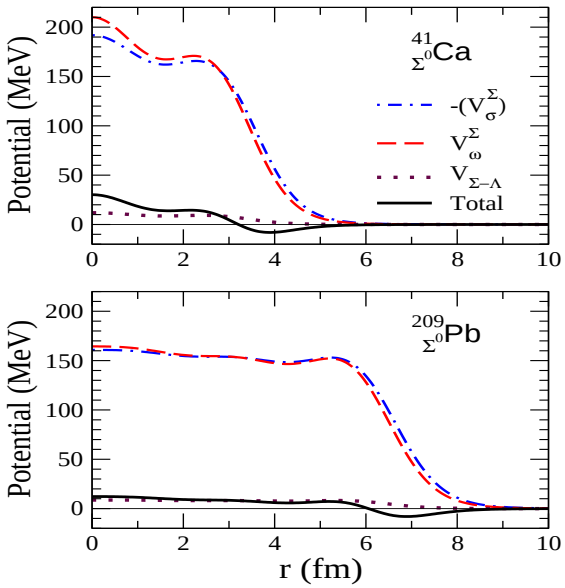

FIGURE 2. Σ^0 potentials in ${}^{41}_{\Sigma^0}$Ca and ${}^{209}_{\Sigma^0}$Pb. See also Refs. [4, 9] for detail.

While the exact numerical values depend on the mass taken for the σ meson, we stress the similarity to the phenomenological form found by Batty *et al.* [12]. For a recent review see [13]. It will clearly be very interesting to pursue the application of the current theoretical formulation to Σ^--atoms.

We also note that this model supports the existence of a variety of bound Ξ hypernuclei. For the Ξ^0 the binding of the 1s level varies from 5 MeV in ${}^{17}_{\Xi^0}$O to 15 MeV in ${}^{209}_{\Xi^0}$Pb. The experimental search for such states at facilities such as J-PARC and GSI-FAIR will be very important.

CONCLUSION

First, the inclusion of the effect of the medium on the one-gluon exchange color magnetic hyperfine interaction between quarks within the quark-meson coupling model (QMC-III), has led to some important advances. This is based on the quark and gluon

dynamics, and it would be non-trivial task for usual SU(3) symmetry and hadron based relativistic mean field approaches to accommodate such effects leading to the absence of middle and heavier mass Σ hypernuclei.

Second, the agreement between the parameter free calculations and the low-lying experimental energy levels for the Λ hypernuclei is impressive, especially between the calculated (-26.9 MeV in ${}^{209}_{\Lambda}$Pb) and the experimental (-26.3 ± 0.8 MeV in ${}^{208}_{\Lambda}$Pb) single-particle energy of the Λ in the $1s_{1/2}$ level. However, for the d- and f-wave levels shown in Table 2, there is a tendency for the model to overbind by several MeV. Whether this is a consequence of the use of an extreme single particle shell model for the core, the omission of residual $\Lambda - N$ interactions or an aspect of the current implementation in QMC-III that requires improvement remains to be seen.

Third, a number of Ξ hypernuclei are predicted to be bound, although not as deeply as in the Λ case.

Last, we emphasize again that the additional repulsion arising from the enhancement of the hyperfine repulsion in the Σ-hyperon in-medium, together with the effect of the $\Sigma N - \Lambda N$ channel coupling on the intermediate range scalar attraction, means that no middle and heavy mass Σ hypernuclei are predicted to be bound. This encouraging picture of finite hypernuclei, suggests that the underlying model, which is fully relativistic and incorporates the quark substructure of the baryons, is ideally suited for application to the properties of dense matter and neutron stars.

ACKNOWLEDGMENTS

KT would like to acknowledge CSSM for hospitality, and thank A. W. Thomas for many exciting collaborations, and celebrate his 60th birthday! Notice: Authored by Jefferson Science Associates, LLC under U.S. DOE Contract No. DE-AC05-06OR23177. The U.S. Government retains a non-exclusive, paid-up, irrevocable, world-wide license to publish or reproduce this manuscript for U.S. Government purposes.

REFERENCES

1. For example, O. Hashimoto and H. Tamura, *Prog. Part. Nucl. Phys.* **57**, 564 (2006).
2. P. K. Saha *et al.*, *Phys. Rev. C* **70**, 044613 (2004).
3. J. Rikovska-Stone, P. A. M. Guichon, H. H. Matevosyan and A. W. Thomas, *Nucl. Phys. A* **792**, 341 (2007).
4. P. A. M. Guichon, A. W. Thomas and K. Tsushima, *Nucl. Phys. A* **814**, 66 (2008).
5. K. Saito, K. Tsushima and A. W. Thomas, *Phys. Rev. C* **55**, 2637 (1997).
6. P. A. M. Guichon, *Phys. Lett. B* **200**, 235 (1988).
7. For a review, K. Saito, K. Tsushima and A. W. Thomas, *Prog. Part. Nucl. Phys.* **58**, 1 (2007).
8. K. Tsushima and F. C. Khanna, *Phys. Lett. B* **552**, 138 (2003).
9. K. Tsushima, K. Saito, J. Haidenbauer and A. W. Thomas, *Nucl. Phys. A* **630**, 691 (1998); K. Tsushima, K. Saito and A. W. Thomas, *Phys. Lett. B* **411**, 9 (1997) [*Erratum-ibid. B* **421**, 413 (1998)].
10. A. Reuber, K. Holinde and J. Speth, *Nucl. Phys. A* **570**, 543 (1994).
11. P. H. Pile et al., *Phys. Rev. Lett.* **66**, 2585 (1991).
12. C. J. Batty, E. Friedman and A. Gal, *Prog. Theor. Phys. Suppl.* **117**, 227 (1994).
13. E. Friedman and A. Gal, *Phys. Rep.* **452**, 89 (2007).